Vol 17 No 12, December 2008
1674-1056/2008/17(12)/4606-08

Chinese Physics B

© 2008 Chin. Phys. Soc.
and IOP Publishing Ltd

Hydrostatic pressure effect on the electron mobility in a ZnSe/$Zn_{1-x}Cd_xSe$ strained heterojunction*

Bai Xian-Ping(白鲜萍)† and Ban Shi-Liang(班士良)

Department of Physics, School of Physical Science and Technology, Inner Mongolia University, Hohhot 010021, *China*

(Received 12 May 2008; revised manuscript received 21 May 2008)

With a memory function approach, this paper investigates the electronic mobility parallel to the interface in a ZnSe/$Zn_{1-x}Cd_xSe$ strained heterojunction under hydrostatic pressure by considering the intersubband and intrasubband scattering from the optical phonon modes. A triangular potential approximation is adopted to simplify the potential of the conduction band bending in the channel side and the electronic penetrating into the barrier is considered by a finite interface potential in the adopted model. The numerical results with and without strain effect are compared and analysed. Meanwhile, the properties of electronic mobility under pressure versus temperature, Cd concentration and electronic density are also given and discussed, respectively. It shows that the strain effect lowers the mobility of electrons while the hydrostatic pressure effect is more obvious to decrease the mobility. The contribution induced by the longitudinal optical phonons in the channel side is dominant to decide the mobility. Compared with the intrasubband scattering it finds that the effect of intersubband scattering is also important for the studied material.

Keywords: electron mobility, ZnSe/$Zn_{1-x}Cd_xSe$, strain, pressure effect
PACC: 6320K, 7220D, 7340L

1. Introduction

The electrical and optical properties of strained heterostructures consisting of the II–VI group with wide-band-gap materials such as ZnSe/$Zn_{1-x}Cd_xSe$ have been studied both theoretically and experimentally due to their potential application in blue lasers, light-emitting diodes and so on.[1−3] In an early year, the change of electron energy and the variation of the band gap induced by the biaxial in-plane strain due to the interface mismatch of lattice constants were studied for ZnSe/$Zn_{1-x}Cd_xSe$ strained quantum wells.[1] More recently, the shift of phonon frequencies and the variation of electron-phonon interaction were discussed to emphasize the strain effect.[4]

On the other hand, as a useful tool hydrostatic pressure is widely used to probe and modulate the physical properties of the low-dimensional semiconductor systems.[5−8] The previous results showed that the hydrostatic pressure affects obviously the electronic effective mass, energy band gap,[5] dielectric constants, frequencies of optical phonons,[6,7]and the cyclotron mass of an electron with phonon effect,[8] etc. Thus, a deeper understanding about pressure modulation on the physical parameters of heterostructures with strain effect is also helpful both in theoretical development and device designment.

In recent decades, the electron mobility in heterostructures has become a subject intensively investigated with the quick development of microstructure science and technology. Hasbun *et al*[9] adopted a memory function approach to discuss the temperature-dependent electron mobility in a two-dimensional (2D) $Al_xGa_{1-x}As$/GaAs heterojunction due to the scattering from optical phonons. We found that the phonon scattering in a quasi 2D system is stronger than that in a 3D one. The theoretical calculation of electron mobility as a function of electronic density was presented by Ridley *et al*[10] in $Al_xGa_{1-x}N$/GaN heterostructures considering the scattering from interface and half-space optical modes using the Boltzmann equation. Their result showed that the 2D mobility is significantly greater than the bulk mobility. Moreover, we[11] studied the hydrostatic pressure effect on the mobility of electrons in $Al_xGa_{1-x}As$/GaAs heterojunctions by neglecting the intersubband scattering on electrons and showed that the mobility decreases with increasing pressure. And Hao *et al*[12] also discussed the electron mobility under

*Project supported by the National Natural Science Foundation (Grant No 60566002) and the Specialized Research Fund for the Doctoral Program of Higher Education (Grant No 20070126001) of China.
†E-mail: ndbaixp@imu.edu.cn

pressure in AlAs/GaAs quantum wells with force balance equation to clarify the roles of various branches of phonons. However, most literatures on the electron mobility are related mainly to the III–V group[9,11−14] or III–N[10,15,16] materials, and neglect the effect of ternary mixed crystals (TMCs) especially on the interface phonons, whereas the II–VI group materials were studied scarcely up to now. Detailed studies of electron mobility in such strained-layer semiconductors are of benefit to explore their application in quantum cascade lasers and high electron mobility transistors.

This paper discusses the electronic mobility influenced by optical phonons with a memory function approach by considering the biaxial in-plane strain and hydrostatic pressure effects within the temperature range that the optical phonon scattering is dominant. The influences of intersubband and intrasubband scattering on electrons are also taken into account using a triangle potential model to approximate the subbands induced by the energy band bending and finite interface barrier. Under pressure the dependence of the electronic mobility on temperature, Cd concentration and electronic density are given and discussed, respectively.

2. Theory and model

We consider a heterojunction consisting of two different polar semiconductors, for which the channel side $Zn_{1-x}Cd_xSe$ denoted by material 1 is located at $z > 0$ and the barrier side ZnSe denoted by material 2 is located at $z < 0$, respectively. The interface of the heterojunction is chosen as the $x - y$ plane, which is assumed to be infinite without losing generality.

In the system, there are two types of optical phonons interacting with electrons: the two branches of interface optical (IO) phonons with high and low frequencies $\omega_{\pm}$, and the two branches of bulk longitudinal optical (LO) phonons with frequency ω_{L1} and ω_{L2} in the channel and barrier layers, respectively.

2.1. Electron eigenfunction

In an effective mass approximation, the electronic wave function of subband n for the studied system can be described by

$$\Psi_k(\boldsymbol{\rho}, z) = \frac{1}{\sqrt{A}} \exp\left[\mathrm{i}\left(\boldsymbol{k}\cdot\boldsymbol{\rho}\right)\right] \psi_n(z), \tag{1}$$

where A is the area of sample, $\boldsymbol{k} = (k_x, k_y)$ and $\boldsymbol{\rho} = (x, y)$ are the wave vector and coordinate vector in the $x - y$ plane for the 2D electronic gas, respectively.

Adopting the triangle potential approximation to simplify the interface potential and energy band bending in the channel side,[17] we can obtain the n-th subband eigenfunction $\psi_n(z)$ in the z direction by solving the following equations

$$\begin{aligned} &-\frac{\hbar^2}{2m_1^*}\frac{\partial^2}{\partial z^2}\psi_n(z) + eF_z z\psi_n(z) = E_n\psi_n(z), z > 0 \\ &-\frac{\hbar^2}{2m_2^*}\frac{\partial^2}{\partial z^2}\psi_n(z) + \Delta E_C\psi_n(z) = E_n\psi_n(z), z \le 0 \end{aligned} \tag{2}$$

where E_n is the n-th subband energy eigenvalue of electrons. $F_z = 4\pi e n_s/\varepsilon_{01}$ is an electric field induced by conduction band bending in the channel side, n_s is the electronic density. The conduction band offset $\Delta E_C$is assumed to be 0.7 times the band gap difference of the two materials consisting of the heterojunction.[18]

2.2. Hamiltonian of the electron -phonon interaction and its matrixes

The quantized Hamiltonian with electron–phonon interaction in a quasi 2D ZnSe/$Zn_{1-x}Cd_xSe$ heterojunction can be written as[9]

$$\begin{aligned} H_{\mathrm{e-ph}} = &\sum_{n_1,n_2,Q,\lambda} M(n_1, n_2, q, q_z, \lambda) \exp\left(\mathrm{i}\boldsymbol{q}\cdot\boldsymbol{R}\right) \\ &\times \left(b_{Q,L\lambda} + b^{\dagger}_{-Q,L\lambda}\right)\rho_q \\ &+ \sum_{n_1,n_2,q,\sigma} M(n_1, n_2, q, \sigma) \exp\left(\mathrm{i}\boldsymbol{q}\cdot\boldsymbol{R}\right) \\ &\times \left(a_{q,\sigma} + a^{\dagger}_{-q,\sigma}\right)\rho_q, \end{aligned} \tag{3}$$

where $\rho_q = C^{+}_{k+q}C_k$ is the electronic density operator, $n_1, n_2 = 0, 1$ represent the subband indices, $Q = \sqrt{q^2 + q_z^2}$ is the wave vector of an optical phonon, $b_{Q,L\lambda}, a_{q,\sigma}$ and $b^{\dagger}_{Q,L\lambda}, a^{\dagger}_{q,\sigma}$ are the annihilation and creation operators of bulk LO for material λ and IO phonons, respectively, here $\lambda = 1, 2$ and $\sigma = \pm$.

Here the Fröhlich interaction matrices between subbands n_1 and n_2 coupling with the LO and IO phonons are defined as $M(n_1, n_2, \boldsymbol{q}, q_z, \lambda) = M_\lambda(\boldsymbol{q}, q_z)I(n_1, n_2, q_z)$ and $M(n_1, n_2, \boldsymbol{q}, \sigma) = A(\boldsymbol{q}, \sigma)J(n_1, n_2, q)$, where, the coupling strengths $M_\lambda(\boldsymbol{q}, q_z)$ and $A(\boldsymbol{q}, \sigma)$ are given respectively by

$$M_\lambda(\boldsymbol{q}, q_z) = \mathrm{i}\left[\frac{e^2}{\varepsilon V}\hbar\omega_{L\lambda}\left(\frac{1}{\varepsilon_{\infty\lambda}} - \frac{1}{\varepsilon_{0\lambda}}\right)\right]^{1/2}\frac{1}{Q}, \tag{4}$$

and

$$A(\boldsymbol{q},\sigma)=\mathrm{i}\frac{1}{\sqrt{q}}\left(\frac{\hbar e^2}{2A\omega_\sigma\varepsilon(\delta_{1\sigma}^2+\delta_{2\sigma}^2)}\right)^{1/2}. \quad (5)$$

Furthermore, the matrix elements $I(n_1,n_2,q_z)$ and $J(n_1,n_2,q)$ are respectively expressed as

$$I(n_1,n_2,q_z)=\int_{-\infty}^{\infty}\psi_{n_1}(z)\psi_{n_2}^*(z)\sin(q_z z)\,\mathrm{d}z, \quad (6)$$

and

$$J(n_1,n_2,q)=\int_{-\infty}^{\infty}\psi_{n_1}(z)\psi_{n_2}^*(z)\exp(-q|z|)\,\mathrm{d}z, \quad (7)$$

where $\delta_{\lambda\sigma}=\dfrac{(\varepsilon_{0\lambda}-\varepsilon_{\infty\lambda})^{1/2}\omega_{T\lambda}}{(\omega_{T\lambda}^2-\omega_\sigma^2)}$. The frequency ω_σ for the σ'th branch of IO phonons can be given by

$$\omega_\pm^2=\frac{b\pm\sqrt{b^2-4ac}}{2a}, \quad (8)$$

where parameters a,b,c depend on the frequencies of LO phonons and transverse optical (TO) phonons for material λ and relate to the Cd concentration.[19]

In the above equations, V is the volume of the material; $\varepsilon,\varepsilon_{\infty\lambda}$ and $\varepsilon_{0\lambda}$ are the vacuum, high frequency and static dielectric constants respectively; $\omega_{T\lambda}$ is the frequency of a TO phonon for material λ.

2.3. Electronic mobility

With a memory function approach,[9] the electron mobility μ considering intersubband and intrasubband scattering by the LO and IO phonons can be given as

$$\frac{1}{\mu}=\frac{2\hbar}{k_{\mathrm{B}}TNe}\left[\sum_{n_1,n_2,Q,\lambda}|M(n_1,n_2,\boldsymbol{q},q_z,\lambda)|^2q_x^2n'\left(\frac{\hbar\omega_{L\lambda}}{k_{\mathrm{B}}T}\right)\Pi_{02}(n_1,n_2,q,\omega_{L\lambda})\right.$$
$$\left.+\sum_{n_1,n_2,\boldsymbol{q},\sigma}|M(n_1,n_2,\boldsymbol{q},\sigma)|^2q_x^2n'\left(\frac{\hbar\omega_\sigma}{k_{\mathrm{B}}T}\right)\Pi_{02}(n_1,n_2,q,\omega_\sigma)\right] \quad (9)$$

The first term on the right-hand side of Eq.(9) represents the contribution from the interaction of electron-LO phonons, and the second one is the contribution from that of electron-IO phonons. In Eq.(9), $n'(x)$ is the derivative of the phonon number with respect to x. Π_{02} is the imaginary part of the 2D density–density correlation function.[14]

3. Biaxial strain and pressure effects

In order to obtain the biaxial in-plane strain and the hydrostatic pressure effects on the mobility of electrons in such a heterojunction, we need to discuss the dependence of lattice constants, electronic effective mass, dielectric constants, phonon frequencies and energy band gaps on both the biaxial strain and hydrostatic pressure.

According to the Murnaghan's state equation,[2] the lattice constant of material λ in the low-pressure region are determined by

$$a_\lambda(p)=a_{0\lambda}\left(1-\frac{p}{3B_{0\lambda}}\right), \quad (10)$$

where $B_{0\lambda}$ is the bulk modulus, $a_{0\lambda}$ is the lattice constant in the absence of strain.

Both the biaxial lattice-mismatch-induced strain and the contribution from hydrostatic pressure to the total strain of the materials are given as [2,4]

$$\bar{\epsilon}_\lambda=\epsilon_{ij\lambda}^h+\epsilon_{ij\lambda}^b, \quad (11)$$

where the hydrostatic pressure components satisfy

$$\epsilon_{ij\lambda}^h=\epsilon_{xx\lambda}^h=\epsilon_{yy\lambda}^h=\epsilon_{zz\lambda}^h$$
$$=\frac{a_\lambda(p)-a_{0\lambda}}{a_{0\lambda}}=-\frac{p}{3B_{0\lambda}}, \quad (12)$$

and the biaxial strain components are given by

$$\epsilon_{xx1}^b=\epsilon_{yy1}^b=\frac{a_2(p)-a_1(p)}{a_1(p)}=\epsilon_1^b(p),$$
$$\epsilon_{xx2}^b=\epsilon_{yy2}^b=\frac{a_1(p)-a_2(p)}{a_2(p)}=\epsilon_2^b(p), \quad (13)$$

for the channel and barrier layers, respectively. Furthermore,

$$\epsilon_{zz\lambda}^b=-\frac{2C_{12\lambda}}{C_{11\lambda}}\epsilon_\lambda^b(p),\ \epsilon_{xy\lambda}^b=\epsilon_{yz\lambda}^b=\epsilon_{zx\lambda}^b=0, \quad (14)$$

where C_{11} and C_{12} are the elastic constants.

From Eqs.(10) to (15), the change of fractional volume due to the biaxial strain and hydrostatic pressure can be expressed as [2]

$$\left(\frac{\Delta V}{V}\right)_\lambda = \left(\frac{V-V_0}{V}\right)_\lambda = \bar{\in}_{xx\lambda} + \bar{\in}_{yy\lambda} + \bar{\in}_{zz\lambda} = -\frac{p}{B_{0\lambda}} + 2\left(1 - \frac{C_{12\lambda}}{C_{11\lambda}}\right) \in_\lambda^b (p), \quad (15)$$

where V_0 is the volume of the studied material without strain.

The band gap under biaxial strain modulated by hydrostatic pressure is given by[20]

$$E_{g\lambda}(p) = E_{g\lambda}(0) + a_{cv\lambda}\left(\frac{\Delta V}{V}\right)_\lambda, \quad (16)$$

where $a_{cv\lambda}$ is the deformation potential of the band gap at the Γ-point, and $E_{g\lambda}(0)$ is the band gap without strain for material λ.

The strain-dependent electronic effective mass is given by[21]

$$\frac{m_{0\lambda}}{m^*_\lambda(p)} = 1 + \frac{A_\lambda}{E_{g\lambda}(p)}, \quad (17)$$

where parameter A_λ is a constant obtained by solving Eq.(17) for $p = 0$.

Furthermore, for the strain dependence of the static dielectric constant, we use the equation given by[4]

$$\varepsilon_{0\lambda}(V) = \varepsilon_{\infty\lambda}(V_0) + [\varepsilon_{0\lambda}(V_0) - \varepsilon_{\infty\lambda}(V_0)] \cdot \left(1 - \left(\frac{\Delta V}{V}\right)_\lambda\right), \quad (18)$$

where $\varepsilon_{0\lambda}(V_0)$ and $\varepsilon_{\infty\lambda}(V_0)$ are the static and the high frequency dielectric constants without strain effect, respectively.

By using the bond–orbital model, we can write the high frequency dielectric constant of strain-dependence as[7]

$$\varepsilon_{\infty\lambda}(V) = 1 + [\varepsilon_{\infty\lambda}(V_0) - 1] \cdot \frac{(V_0/V)^{5/3}_\lambda}{\left\{1 + C_\lambda\left[(V_0/V)^{4/3}_\lambda - 1\right]\right\}^{3/2}}. \quad (19)$$

It can be found that the dielectric constant of high frequency decreases nonlinearly versus strain, where parameter C_λ is a constant and can be derived by

$$C_\lambda = \frac{1}{2}\left[\frac{B_{0\lambda}}{\varepsilon_{\infty\lambda}(V_0) - 1} \cdot \left(-\frac{\partial\varepsilon_{\infty\lambda}(p)}{\partial p}\right)_{p=0} + \frac{5}{3}\right]. \quad (20)$$

The derivative in Eq.(20) can be obtained using the formula given by Goni *et al*[22]

$$\frac{\partial \ln \varepsilon_{\infty\lambda}(p)}{\partial \ln V} = \frac{5\left[\varepsilon_{\infty\lambda}(p) - 1\right]}{3\varepsilon_{\infty\lambda}(p)}(0.9 - f_{i\lambda}), \quad (21)$$

where $f_{i\lambda}$ is the ionicity of material λ under pressure. Material volume V satisfies approximately the following linear relation:[23]

$$B(p) = -V\frac{\partial p}{\partial V} = B_{0\lambda} + B'_{0\lambda}p. \quad (22)$$

Here B is the bulk modulus and may be assumed as linear with respect to pressure for a lower pressure, and $B'_{0\lambda} = \mathrm{d}B/\mathrm{d}p$ is the first order pressure derivative at zero pressure. For ZnSe and CdSe, the values of B'_0 are 4.77 and 5.3, respectively.[24,25]

According to Refs.[26] and [27], the strain-dependent frequencies of optical phonons can be determined by

$$\omega_{L\lambda}(p) = \omega_{L\lambda}(0) + 2\Delta\Omega_{H\lambda} - \frac{2}{3}\Delta\Omega_{L\lambda}, \quad (23)$$

and

$$\omega_{T\lambda}(p) = \omega_{T\lambda}(0) + 2\Delta\Omega_{H\lambda} + \frac{2}{3}\Delta\Omega_{T\lambda}. \quad (24)$$

In the above two equations

$$\Delta\Omega_{H\lambda} = -\gamma \cdot \frac{s_{11\lambda} + 2s_{12\lambda}}{s_{11\lambda} + s_{12\lambda}}\omega_{L\lambda(T\lambda)}(0)\,\bar{\in}_{xx\lambda}, \quad (25)$$

and

$$\Delta\Omega_{L\lambda(T\lambda)} = a_s \cdot \frac{s_{11\lambda} - s_{12\lambda}}{s_{11\lambda} + s_{12\lambda}}\omega_{L\lambda(T\lambda)}(0)\,\bar{\in}_{xx\lambda}, \quad (26)$$

where s_{11} and s_{12} are the compliance constants, γ is the mode-Grüneisen parameter, and a_s is the shear deformation parameter.

4. Results and discussion

The numerical calculation is performed for ZnSe/$Zn_{1-x}Cd_xSe$ strained heterojunctions, where the tensile strain ($\in > 0$) and compressive strain ($\in < 0$) occur in the ZnSe and $Zn_{1-x}Cd_xSe$ layers respectively. The lattice mismatch between $Zn_{1-x}Cd_xSe$ and ZnSe is within the range from 0 to 6.3% when the Cd concentration in the TMC $Zn_{1-x}Cd_xSe$ varies from 0 to 1. It should be noted that parameters γ and a_s mentioned above corresponding to the TO phonons are taken to be approximately the same as those of the LO phonons. For material $Zn_{1-x}Cd_xSe$ or CdSe, a_s is not available so that $a_{s2} = a_{s1}$ was adopted as an approximation in our computation.

The parameters used in the computation are listed in Tables 1 and 2. Some parameters of the TMC are obtained by a simplified coherent potential approximation.[28] The calculated results are shown in Figs.1–5, respectively.

Table 1. Parameters of ZnSe and CdSe used in computation.

Quantities	ZnSe (A)	CdSe (B)	Quantities	ZnSe (A)	CdSe (B)
a_0/nm	0.5669[a]	0.6052[a]	C_{11}/GPa	82.6[c]	66.7[c]
B_0/GPa	62.4[a]	53.0[a]	C_{12}/GPa	49.8[c]	46.3[c]
m^*/m_0	0.17[b]	0.13[b]	ε_∞	5.9[b]	5.98[b]
E_g/eV	2.821[c]	1.765[c]	ε_0	8.1[b]	9.6[b]
a_{cv}/eV	–4.37[d]	-3.664[d]	$\hbar\omega_L$/meV	31[b]	27[b]
f_i	0.63[e]	0.70[e]	$\hbar\omega_T$/meV	26.457[b]	21.3[b]
$S_{11}/(10^{-11}\,\mathrm{N^{-1}m^2})$	2.26[f]	2.34[g]	γ	1.8[f]	1.3[h]
$S_{12}/(10^{-11}\,\mathrm{N^{-1}m^2})$	–0.85[f]	–1.12[g]	a_s	0.62[f]	

[a] Ref.[24]; [b] Ref.[28]; [c] Ref.[3]; [d] Ref.[1]; [e] Ref.[29]; [f] Ref.[30]; [g] Ref.[31]; [h] Ref.[32].

Table 2. Parameters of $Zn_{1-x}Cd_xSe$ used in computation.

Quantities	$Zn_{1-x}Cd_xSe$
E_g/eV	$E_{gA}E_{gB}/(E_{gB}(1-x)+xE_{gA})$
ε_0	$\left[\left((1-x)\,m_B^*\varepsilon_{0A}^2+xm_A^*\varepsilon_{0B}^2\right)\left(x/m_A^*+(1-x)\,/m_B^*\right)\right]^{1/2}$
ε_∞	$\left[\left((1-x)\,m_B^*\varepsilon_{\infty A}^2+xm_A^*\varepsilon_{\infty B}^2\right)\left(x/m_A^*+(1-x)\,/m_B^*\right)\right]^{1/2}$
$\hbar\omega_L$/meV	$\hbar\omega_{LA}\omega_{LB}/\left(\omega_{LB}(1-x)+x\omega_{LA}\right)$
$\hbar\omega_T$/meV	$\hbar\omega_{TA}\omega_{TB}/\left(\omega_{TB}(1-x)+x\omega_{TA}\right)$

Figure 1 shows the dependence of electron mobility μ on temperature T for the given electronic density and Cd concentration, corresponding to without, with the biaxial strain effect, and with the combination of the biaxial strain and hydrostatic pressure effects ($p = 4$ GPa), respectively. The result indicates that μ decreases by the biaxial strain, and the modulation by hydrostatic pressure is more obvious for a lower T. Comparing the numerical results of the three cases, we can see that the net decreases of the mobility are about 8.5% by the strain effect, and from 28.4% to 32.5% by both the strain and pressure effects at T from 200 K to 400 K, respectively. In the $Zn_xCd_{1-x}Se$ channel side, the electronic effective mass and the frequency of phonons increase with the compressive strain induced by the lattice mismatch while the high dielectric constant decreases. The changes of electronic effective mass and dielectric constant decrease μ, whereas μ increases with the frequency of phonons. The competition of the two aspects results in the decrease of μ. However, the case is contrary for ZnSe barrier side because of the tensile strain. The numerical results show that the electronic effective mass plays a dominant role among the above pressure-dependent parameters. We also found that the contribution from the LO phonons in the channel side to the electron mobility is dominant in deciding the total mobility since the penetrating of the electron into the barrier is small. Moreover, the hydrostatic pressure effect strengthens this drop of the mobility with compressive strain.

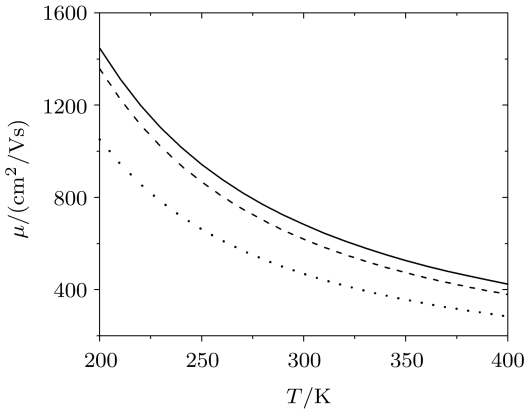


Fig.1. Electronic mobility as a function of temperature T for the given electronic density $n_s = 4.0 \times 10^{11}/\mathrm{cm^2}$ and Cd concentration $x = 0.6$ with the solid, dashed and dot lines corresponding to without, with the biaxial strain effect and with both the effects of the biaxial strain and hydrostatic pressure ($p = 4$ GPa), respectively.

Figure 2 gives μ as a function of hydrostatic pressure p considering the intrasubband and intersubband scattering, respectively. We can see that μ decreases with p and the nonlinearity of mobility due to the scattering of intersubband is similar to that of intrasubband. In the calculated pressure range from 0 to 10 GPa, the net decreases of μ are 46.8%, 45.6% and

46.3% for the intrasubband, intersubband and considering both the intrasubband and intersubband scattering respectively. The p dependences of the electronic effective mass, optical phonon frequencies, and the dielectric constants combine together to influence the energy band bending, interface potential and furthermore the intrinsic properties of the materials influencing on μ. The net increases of the electronic effective mass, band gap and the optical phonon energy in $Zn_{0.4}Cd_{0.6}Se$ are 24.7%, 30.6% and 8.3% respectively, while the net decreases of the lattice constant and the high frequency dielectric constant are 5.8% and 2.5% respectively when p increases to 10GPa from 0. Our calculation shows that both the electronic effective mass and lattice constant are more important, while the static dielectric constant is unimportant under pressure. μ decreases with increasing the electronic effective mass, and the influence of the optical phonon energy in $Zn_{0.4}Cd_{0.6}Se$ counterbalances the decrease. As a result, the pressure-induced reduction of the electron mobility results from their combination effect. But the change of the electronic effective mass is more significant to decide μ.

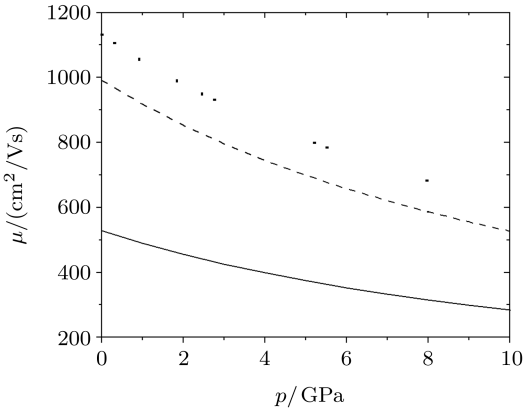


Fig.2. Electron mobility as a function of hydrostatic pressure p due to intrasubband (dashed line) and intersubband (dot line) scattering for the given temperature $T = 300\,\mathrm{K}$ and Cd concentration $x = 0.6$, respectively. The total mobility from 'intra + inter'-subband scattering is denoted by the solid line and described by $\mu_T^{-1} = \mu_{\mathrm{intra}}^{-1} + \mu_{\mathrm{inter}}^{-1}$.

Meanwhile, Fig.2 shows that although the intrasubband scattering is dominant, the intersubband scattering is also important. The numerical calculation indicates that the contribution from the intrasubband scattering to the total mobility is about 60%, and the intersubband scattering is about 40%. It is expected that the latter may be more important for real conduction band bending instead of our triangular potential approximation. It should be noted that the proportion of intrasubband scattering in the total mobility is promoted gradually with the increase of p.

In Fig.3, the change of μ with Cd concentration x due to intrasubband and intersubband scattering is presented for the given $T = 300\,\mathrm{K}$, $p = 4\,\mathrm{GPa}$ and different electronic densities. For comparison, the corresponding curves are also given for $p = 0$, respectively. The concentration-induced trend of the total mobility is similar to that of intrasubband and intersubband. Comparing Fig.3(a) with Fig.3(b), we find that the Cd concentration-dependent μ for higher n_s is different from that of lower n_s. Figure 3(a) shows that the mobility decreases to a minimum point and then increases with x. This attributes mainly to the competition between the electron-phonon coupling strength and the electronic density correlation effect described by the electronic density correlation function $\Pi_{02}(n_1, n_2, q, \omega)$. With increasing x from 0, the electronic effective mass and the frequency of phonons decrease while the high dielectric constant and biaxial strain effect increase. The combination of these factors makes the electron-phonon coupling constant becoming larger while the correlation effect of electrons decreases. As a result, the net decreases of μ due to the former and the biaxial strain effect go beyond the net increase due to the latter, and the mobility drops. However, for larger x, the influence induced by the decreasing of electronic effective mass plays a main role to diminish the density correlation effect. This influence is superior to the effect of the electron-phonon coupling and results in the upward trend of μ. As for Fig.3(b), the 2D property of the heterojunction with a higher electronic density is stronger than the other factors to weaken the scattering from LO phonons. The scattering from the IO phonons becomes slightly strong but it cannot counteract the decrease of the scattering from the LO phonons so that the total mobility is bigger than that of Fig.3(a) in the whole range of x. Meanwhile, the large density correlation effect of electrons induced by the higher n_s decreases μ as increase of x. Figure 3 also shows that the pressure effect is more obvious for less (larger) x as $n_s$increases (decreases) to decrease the mobility.

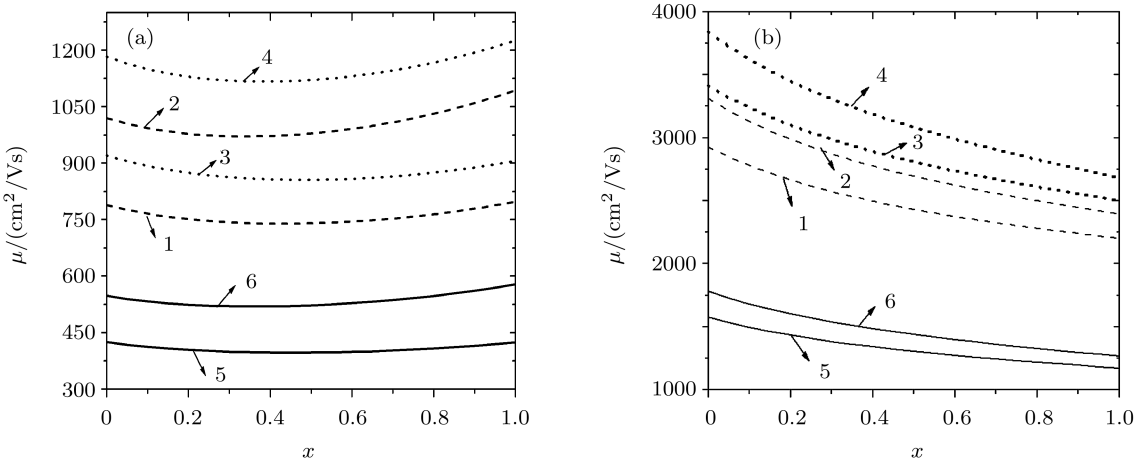


Fig.3. Electron mobility as a function of Cd concentration x due to intrasubband and intersubband scattering for the given temperature $T = 300\,\mathrm{K}$ and different electronic density (a) $n_s = 4.0 \times 10^{11}/\mathrm{cm}^2$, (b) $n_s = 80.0 \times 10^{11}/\mathrm{cm}^2$, respectively. Curves 1(2), 3(4) and 5(6) indicate the scattering from intrasubband, intersubband and 'intra + inter'-subband corresponding to $p = 4$ (0) GPa, respectively.

In Fig.4, the contributions to the mobility from the intrasubband, intersubband and from both of the intrasubband and intersubband scattering are given as functions of n_s under $p = 4\,\mathrm{GPa}$ at $T = 300\,\mathrm{K}$. From Fig.4 one can see that the mobility increases to a maximum value and then dramatically decreases as n_s increases. At low n_s, the mobility is determined mainly by the strong scattering from the LO phonon modes since the confinement and correlation of electrons are both weak. Increasing n_s induces the band bending so that the average distance of electrons to the interface decreases. As discussed above, the scattering from the IO phonons becomes slightly strong but it cannot counteract the decrease of the scattering from the LO phonons so that the total mobility increases firstly and gives rise a maximum to the mobility. At much large n_s, the strong correlation of the electrons reduces obviously the mobility as n_s increases.

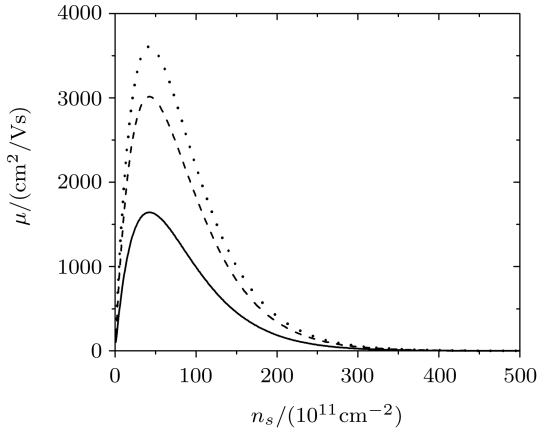


Fig.4. Electron mobility as a function of electronic density n_s due to intrasubband (dashed line) and intersubband (dot line) scattering for the given temperature $T = 300\,\mathrm{K}$, pressure $p = 4\,\mathrm{GPa}$ and Cd concentration $x = 0.6$, respectively. The total mobility from 'intra + inter'-subband scattering is denoted by the solid line.

Here, the same conclusion as Fig.2 can be obtained for the contributions of the intrasubband and intersubband scattering to the total mobility.

The contributions to the electron mobility from the scattering of the IO and LO phonons are plotted as a function of n_s at $T = 300\,\mathrm{K}$ in Fig.5, considering both the intrasubband and intersubband transition corresponding to $p = 4\,\mathrm{GPa}$ and 0, respectively. It shows that the contribution to μ from the LO phonons is dominant so that the mobility is nearly coincident with the total mobility. As discussed above, the effect of electronic density correlation plays an important role to decide the mobility. It should be noted that the contribution from the IO phonons can be neglected for wide-band semiconductors and the conclusion is opposite for the III–V group semiconductors.[11] The contribution from the LO phonons in the barrier has been also computed for different n_s and the result indicates that its scattering can be neglected although it is larger than that from the IO phonons. Meanwhile, Fig.5 indicates that the hydrostatic pressure reduces the increase of the mobility at less n_s, while reduces its decrease at higher n_s. For less n_s, the coupling between electrons and phonons becomes stronger under pressure than that without pressure to result in the less mobility. As for larger n_s, the decrease of the

correlation of electrons due to the modulation from

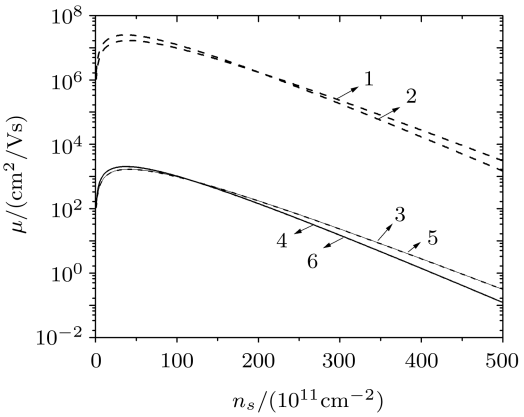


Fig.5. Electron mobility considering the 'intra + inter'-subband scattering as a function of electronic density n_s due to the IO and LO phonons for the given temperature $T = 300\,\mathrm{K}$ and Cd concentration $x = 0.6$. Curves 1(2), 3(4) and 5(6) indicate the contributions from IO, LO and IO+LO phonons corresponding to pressure $p = 4$ (0) GPa, respectively.

pressure plays a dominant role to raise the mobility in comparison with that without the modulation.

5. Conclusions

We discuss the hydrostatic pressure effect on the electron mobility in a strained $ZnSe/Zn_{1-x}Cd_xSe$ heterojunction with finite barrier by considering the intrasubband and intersubband scattering from optical phonons. The results show that the electron mobility decreases with the increase of hydrostatic pressure and the biaxial strain. Furthermore, the strain-induced reduction of electron mobility is obvious and needs to be considered for further work. The intersubband scattering is also important in comparison with the intrasubband scattering and is not negligible. Meanwhile, the scattering from the bulk LO phonons in the channel side is dominant to decide the electron mobility.

References

[1] Lozykowski H J and Shastri V K 1991 *J. Appl. Phys.* **69** 3235

[2] Tuchman J A, Kim S, Sui Z and Herman I P 1992 *Phys. Rev.* B **46** 13371

[3] Cingolani R, Prete P, Greco D, Giugno P V, Lomascolo M, Rinaldi R and Calcagnile L 1995 *Phys. Rev.* B **51** 5176

[4] Guo Z Z, Liang X X and Ban S L 2003 *Phys. Stat. Sol.* (b) **238** 173

[5] Skierbiszewski C, Perlin P, Wisniewski P, Suski T, Walukiewicz W, Shan W, Ager J W, Haller E E, Geisz J F, Friedman D J, Olson J M and Kurtz S R 1999 *Phys. Stat. Sol.* (b) **216** 135

[6] Mccluskey M D, Haller E E, Walker J, Johnson N M, Vetterhoffer J, Weber J, Joyce T B and Newman R C 1997 *Phys. Rev.* B **56** 6404

[7] Wagner J M and Bechstedt F 2000 *Phys. Rev.* B **62** 4526

[8] Yu X L and Ban S L 2006 *Eur. Phys. J.* B **52** 483

[9] Hasbun J E and Ban S L 1998 *Phys. Rev.* B **58** 2102

[10] Ridley B K, Foutz B E and Eastman L F 2000 *Phys. Rev.* B **61** 16862

[11] Bai X P and Ban S L 2007 *Eur. Phys. J.* B **58** 31

[12] Hao G D, Ban S L and Jia X M 2007 *Chin. Phys.* **16** 3766

[13] Lei X L, Horing N J M and Cui H L 1992 *Surf. Sci.* **263** 172

[14] Lei X L, Birman J L and Ting C S 1985 *J. Appl. Phys.* **58** 2270

[15] Gurusinghe M N, Davidsson S K and Andersson T G 2005 *Phys. Rev.* B **72** 045316

[16] Farvacque J L and Carosella F 2005 *Phys. Rev.* B **72** 125344

[17] Guo Z Z, Liang X X and Ban S L 2006 *Phys. Scr.* **73** 137

[18] Puls J, Rabe M, Siarkos A and Henneberger F 1998 *Phys. Rev.* B **57** 14749

[19] Ban S L and Hasbun J E 1999 *Phys. Rev.* B **59** 2276

[20] Shahzad K, Olego D J and Van de Walle C G 1988 *Phys. Rev.* B **38** 1417

[21] Ting D Z Y and Chang Y C 1987 *Phys. Rev.* B **36** 4359

[22] Goni A R, Syassen K and Cardona M 1990 *Phys. Rev.* B **41** 10104

[23] Anderson O L 1966 *J. Phys. Chem. Solids* **27** 547

[24] Tuchman J A and Herman I P 1992 *Phys. Rev.* B **45** 11929

[25] Lam P K, Cohen M L and Martinez G 1987 *Phys. Rev.* B **35** 9190

[26] Cerdeira F, Buchenauer C J, Pollak F H and Cardona M 1972 *Phys. Rev.* B **5** 580

[27] Menendez J, Pinczuk A, Valladares J P, Feldman R D and Austin R F 1987 *Appl. Phys. Lett.* **50** 1101

[28] Ban S L and Hasbun J E 1999 *Eur. Phys. J.* B **8** 453

[29] Camphausen D L, Connell G A N and Paul W 1971 *Phys. Rev. Lett.* **26** 184

[30] Pelekanos N T, Ding J, Hagerott M, Nurmikko A V, Luo H, Samarth N and Furdyna J K 1992 *Phys. Rev.* B **45** 6037

[31] Gavini A and Cardona M 1970 *Phys. Rev.* B **1** 672

[32] Reparaz J S, Goni A R, Alonso M I, Perez-Paz M N and Tamargo M C 2006 *Appl. Phys. Lett.* **89** 231109